

## Electron Localization in Alkali-Halide Clusters

Uzi Landman

*School of Physics, Georgia Institute of Technology, Atlanta, Georgia 30332, and Institute of Theoretical Physics, Chalmers University of Technology, 412 96 Goteborg, Sweden*

and

Dafna Scharf and Joshua Jortner

*Department of Chemistry, Tel Aviv University, 69978 Tel Aviv, Israel*

(Received 14 January 1985)

The quantum path-integral molecular-dynamics method was applied to explore the structure, energetics, and dynamics of an excess electron interacting with an alkali-halide cluster. Four distinct modes of electron localization were established, which depend on the cluster composition, size, and structure; they involve an internal *F*-center defect, an external surface state, dissociative detachment of an alkali atom, and structural isomerization induced by electron attachment.

PACS numbers: 71.45.Nt, 36.40.+d, 61.20.Ja

Structural, electronic, dynamic, and chemical characteristics of materials depend primarily on the state (phase) and the degree (size) of aggregation. Small clusters, i.e., finite aggregates containing 3–500 particles, exhibit unique physical and chemical phenomena, which are of both fundamental and technological significance, and provide ways and means to explore the “transition” from molecular to condensed-matter systems.<sup>1</sup> Theoretical studies of clusters were hampered by the relatively large number of particles, which renders the adaptation of molecular science techniques rather cumbersome, while the lack of translational symmetry inhibits the employment of solid-state methodology. Molecular-dynamics (MD) simulations, consisting of the generation of phase-space trajectories via the numerical integration of the (classical) equations of motion for a many-particle system, are particularly suitable for the study of the structure and dynamics of small clusters.<sup>2,3</sup> In this context, localized excess electron states in clusters<sup>4</sup> are of considerable interest with regard to the (nonreactive and reactive) mechanisms of electron attachment, the formation of bulk or surface states, and the role of the excess electron as a probe for the interrogation of the nuclear dynamics of the cluster. Furthermore, quantum phenomena are expected to be pronounced in such systems since the electron wavelength is comparable to the cluster size. In this paper we report on the structure, energetics, and dynamics of alkali-halide clusters (AHC) studied with classical MD, and of electron alkali clusters studied with the quantum path-integral MD method (QUPID).<sup>5–8</sup> AHC were chosen

since the nature of the interionic interactions is well understood and in view of the abundance of model calculations and experimental information of these systems.<sup>9</sup> Our QUPID calculations establish four modes of localization of an excess electron in AHC: (i) an *F*-center defect with the excess electron replacing an internal halide ion; (ii) a new surface state, i.e., a “surface *F* center” of the excess electron; (iii) dissociative electron attachment to AHC resulting in the formation of an “isolated” alkali atom; (iv) structural isomerization induced by electron attachment. Our calculations establish the compositional, structural, and size dependence of these various localization mechanisms.

The QUPID method<sup>6–8</sup> was applied to a system of an electron interacting with an AHC consisting of  $N$  ions ( $N_1$  cations and  $N_2$  anions). The interionic potential energy within the AHC is  $V_{\text{AHC}} = \sum_{IJ} \Phi_{IJ}(R_{IJ})$ , with the interionic pair potentials  $\Phi_{IJ}(R_{IJ})$  being given by the Born-Mayer potential with the parameters determined by Fumi and Tosi.<sup>10</sup> The electron-AHC potential is  $V_e(\mathbf{r}) = \sum_I \Phi_{eI}(\mathbf{r} - \mathbf{R}_I)$  consisting of a sum of electron-ion potentials, which are described by the purely repulsive pseudopotential  $\Phi_{eI}(r) = e^2/r$  for the electron-anion interaction and by the local pseudopotential<sup>11</sup>  $\Phi_{eI}(r) = -e^2/R_c$ ,  $r \leq R_c$ , and  $\Phi_{eI}(r) = -e^2/r$ ,  $r > R_c$ , for the electron-positive-ion interaction. The Hamiltonian is  $H = K_e + V_e + K_{\text{AHC}} + V_{\text{AHC}}$ , where  $K_e$  and  $K_{\text{AHC}}$  are the kinetic-energy operators for the electron (mass  $m$ ) and of the ions (masses  $M_I = M_1$  and  $M_2$ ), respectively. Observables are obtained from the quantum partition function  $Z = \lim_{p \rightarrow \infty} [Z_p]^p$  with

$$Z_p = \text{Tr}[\exp(-\tau K_{\text{AHC}})\exp(-\tau K_e)\exp(-\tau V_{\text{AHC}})\exp(-\tau V_e)],$$

where  $\tau = \beta/p$  and  $\beta = (k_B T)^{-1}$  is the inverse temperature. If we make use of the free particle propagator<sup>12</sup>  $Z_p$  is

$$Z_p = \prod_{\alpha=1,2} \left( \frac{M_\alpha}{2\pi\tau\hbar^2} \right)^{3N_\alpha p/2} \left( \frac{m}{2\pi\tau\hbar^2} \right)^{3p/2} \int \prod_{I=1}^N d^3 R_I \prod_{i=1}^p d^3 r_i \exp[-\beta(V_{\text{eff}}^e + V_{\text{eff}}^I)], \quad (1)$$

where

$$V_{\text{eff}} = \sum_{i=1}^p \left[ \frac{pm}{2\hbar^2\beta^2} (\mathbf{r}_i - \mathbf{r}_{i+1})^2 + V_e(\mathbf{r}_i)/p \right]$$

and

$$V_{\text{eff}}^I = \sum_{l=1}^N \sum_{i=1}^p \frac{pM_l}{2\hbar^2\beta^2} (\mathbf{R}_{l(i)} - \mathbf{R}_{l(i+1)})^2 + V_{\text{AHC}}/p.$$

Equation (1) maps the quantum problem onto the classical statistical mechanics of  $N+1$  particles, each consisting of a periodic chain (necklace) of  $p$  pseudoparticles (beads) with nearest-neighbor harmonic interchain interactions, whose strengths depend upon the masses ( $m, M_1, M_2$ ), the temperature ( $T$ ), and the pseudoparticle number ( $p$ ). When the thermal wavelength [ $\lambda_T = (\beta\hbar^2/M_l)^{1/2}$ ] is smaller than any relevant length scale, the Gaussian factor in  $Z_p$  reduces to a delta function and the necklace collapses

$$H = \sum_{i=1}^p \frac{m^* \dot{\mathbf{r}}_i^2}{2} + \sum_{i=1}^N \frac{M_l \dot{\mathbf{R}}_l^2}{2} + \sum_{i=1}^p \left[ \frac{pm(\mathbf{r}_i - \mathbf{r}_{i+1})^2}{2\hbar^2\beta^2} + \frac{V_e(\mathbf{r}_i)}{p} \right] + V_{\text{AHC}}, \quad (2)$$

the mass  $m^*$  being arbitrary and taken as  $m^* = 1$  u.

Numerical simulations were performed for an electron interacting with sodium-chloride clusters at about room temperature. On the basis of examination of the stability of the variance of the kinetic-energy contribution  $K_{\text{int}}$ , the number of "electron beads" was taken as  $p=399$ . By use of an integration step of  $\Delta t = 1.03 \times 10^{-15}$  sec, long equilibration runs were performed [(1-2)  $\times 10^4 \Delta t$ ]. The reported results were obtained via averaging over  $8 \times 10^3 \Delta t$ , following equilibration. The electron-ion pseudopotential parameters were varied by changing the cutoff radius  $R_c$  in the range (3.22-5.29)  $a_0$ . From QUPID calculations on a single Na atom, the atomic ionization potential is reproduced (see Table I) for  $R_c = 5.29 a_0$ , which seems to be a too-high value for the characterization of this pseudopotential.<sup>6</sup> Therefore, on the basis of pseudopotential parametrization studies<sup>11</sup> and a recent QUPID study<sup>8</sup> of  $F$  centers in molten and solid KCl in which the same form of pseudopotential was employed, a value of  $R_c = 3.22 a_0$  (yielding a value of -0.3005 a.u. for the electron binding energy to  $\text{Na}^+$ , see Table I) is preferred. Fortunately, our conclusions regarding internal and surface-localization modes remain unchanged with respect to reasonable variations of this parameter. In simulations involving the electron-AHC interaction, different initial conditions were employed, two of which for the  $[\text{Na}_{14}\text{Cl}_{13}]^+$  system are portrayed in Figs. 1(a) and 1(b). The resulting final state of the system was found to be independent of the initial conditions.

It has previously been suggested on the basis of zero-temperature structural calculations,<sup>9</sup> and has been confirmed by our classical MD simulations, that when

to a classical particle. This is the case for the ionic part of our system. The average energy of the system is given at equilibrium by

$$E = \frac{3N}{2\beta} + \langle V_{\text{AHC}} \rangle + K_e + p^{-1} \left\langle \sum_{i=1}^p V_e(\mathbf{r}_i) \right\rangle$$

with the electron kinetic energy

$$K_e = \frac{3}{2\beta} + \frac{1}{2p} \sum_{i=1}^p \left\langle \frac{\partial V_e(\mathbf{r}_i)}{\partial \mathbf{r}_i} \cdot (\mathbf{r}_i - \mathbf{r}_p) \right\rangle$$

which consists of the free-particle term ( $3/2\beta$ ) and the contribution from the interaction ( $K_{\text{int}}$ ) with the ions.<sup>13</sup> The statistical averages indicated by angular brackets are over the Boltzmann distributions as defined in Eq. (1). This formalism is converted into a numerical algorithm by noting<sup>14</sup> the equivalence of the sampling described above to that over phase-space trajectories generated via MD by the classical Hamiltonian

the size of the clusters increases ( $N \geq 20$ ), the NaCl crystallographic arrangement is preferred for particular stability for clusters forming rectangular structures even if the number of positive and negative ions is not equal. Therefore, we have chosen to study first the interaction of an electron with  $[\text{Na}_{14}\text{Cl}_{13}]^+$  and  $[\text{Na}_{14}\text{Cl}_{12}]^{++}$  clusters, which exhibit pronounced stability. In Figs. 1(c) and 1(e), we present our results (using  $R_c = 3.22 a_0$ ) for the equilibrium electron-charge distribution obtained from 2D projections of the necklace edge points, and for the nuclear configuration of the clusters. In both cases the electron, which starts in either initial configuration as shown in Figs. 1(a), 1(b), has been localized. However, two distinct modes of electron localizations are exhibited involving *internal* and *external localization* for the doubly charged and singly charged cluster, respectively. The vacancy-containing configuration of the  $[\text{Na}_{14}\text{Cl}_{12}]^{++}$  cluster stabilizes an internally localized excess electron state, with the  $e$  surrounded by six  $\text{Na}^+$  ions in an octahedral configuration and by twelve  $\text{Cl}^-$  ions [Fig. 1(e)] which is similar to the case of an  $F$  center in the extended solid. The electron affinity of the cluster  $E_A = E_B^e + E_c$  is obtained by summing the electron binding energy

$$E_B^e = \frac{3}{2\beta} + K_{\text{int}} + p^{-1} \sum_{i=1}^p \langle V_e(\mathbf{r}_i) \rangle$$

and the cluster reorganization energy  $E_c = \langle V_{\text{AHC}} \rangle - \langle V_{\text{AHC}} \rangle_0$ , where  $\langle V_{\text{AHC}} \rangle_0$  is the potential energy of the "bare" AHC in the absence of the electron. The ionic configuration of the  $e\text{-}[\text{Na}_{14}\text{Cl}_{12}]^{++}$  cluster is somewhat distorted; however, the gain in  $E_B^e$  (-0.249

TABLE I. Average equilibrium temperature ( $\langle T \rangle$ ), interionic cluster potential energy ( $\langle V_{\text{AHC}} \rangle$ ), electron interaction kinetic energy ( $K_{\text{int}}$ ), electron kinetic energy  $K_e = 3/2\beta + K_{\text{int}}$ ,  $e$ -AHC interaction potential energy ( $\langle V_e \rangle$ ), electron binding energy ( $E_{\beta}$ ), cluster reorganization energy ( $E_c$ ), electron affinity of cluster ( $E_A$ ), and Cartesian components of the "electron necklace" gyration radii ( $R_x^2, R_y^2, R_z^2$ ). Atomic units are used (energy and  $\langle T \rangle$  in Hartrees, length in Bohr radii). Variances are given in parentheses. Calculated values of  $\langle T \rangle$  and  $\langle V_{\text{AHC}} \rangle$  for the "bare" clusters:  $[\text{Na}_{14}\text{Cl}_{14}]$ ,  $0.976(0.111) \times 10^{-3}$ ,  $-3.7296$ ;  $[\text{Na}_{14}\text{Cl}_{13}]^+$ ,  $0.948(0.106) \times 10^{-3}$ ,  $-3.5911$ ;  $[\text{Na}_{14}\text{Cl}_{12}]^{++}$ ,  $0.954(0.093) \times 10^{-3}$ ,  $-3.3151$ ;  $[\text{Na}_5\text{Cl}_4]^+$ ,  $1.01(0.38) \times 10^{-3}$ ,  $-1.0999$ .

	$10^3 \langle T \rangle$	$\langle V_{\text{AHC}} \rangle$	$10^2 K_{\text{int}}$	$K_e$	$\langle V_e \rangle$	$E_{\beta}$	$E_c$	$E_A$	$R_x^2$	$R_y^2$	$R_z^2$
$e$ - $[\text{Na}_{14}\text{Cl}_{13}]^+$ $R_c = 3.22$	0.983 (0.035)	-3.4856	6.4195 (0.633)	0.0657	-0.2251	-0.1594	0.1055	-0.0539	5.4	7.0	9.8
$e$ - $[\text{Na}_{14}\text{Cl}_{13}]^+$ $R_c = 5.29$	0.972 (0.031)	-3.5768	1.5182 (0.426)	0.0166	-0.0700	-0.0534	0.0143	-0.0391	23.5	23.2	55.2
$e$ - $[\text{Na}_{14}\text{Cl}_{12}]^{++}$ $R_c = 3.22$	0.938 (0.028)	-3.2372	7.2203 (0.767)	0.0736	-0.3226	-0.2490	0.0799	-0.1691	4.6	6.8	6.3
$e$ - $[\text{Na}_{14}\text{Cl}_{12}]^{++}$ $R_c = 5.29$	0.948 (0.025)	-3.3143	1.9995 (0.956)	0.0214	-0.1365	-0.1151	0.0008	-0.1143	55.3	57.9	43.3
$e$ - $[\text{Na}_5\text{Cl}_4]^+$ $R_c = 3.22$	0.950 (0.132)	-1.0059	2.6389 (0.582)	0.0278	-0.3012	-0.2734	0.0940	-0.1794	2.2	2.0	2.5
$e$ - $[\text{Na}_5\text{Cl}_4]^+$ $R_c = 4.36$	0.946 (0.038)	-1.0483	3.5453 (0.601)	0.0369	-0.1876	-0.1508	0.0516	-0.0992	5.7	7.2	5.5
$e$ - $\text{Na}^+$ $R_c = 3.22$	1.038 (0.442)		0.713 (0.638)	0.0087	-0.3092	-0.3005					$R^2 = 3.6$
$e$ - $\text{Na}^+$ $R_c = 4.36$	1.043 (0.527)		0.034 (0.049)	0.00198	-0.2299	-0.2280					$R^2 = 3.4$
$e$ - $\text{Na}^+$ $R_c = 5.29$	1.084 (0.574)		0.012 (0.032)	0.0017	-0.18897	-0.1872					$R^2 = 4.9$

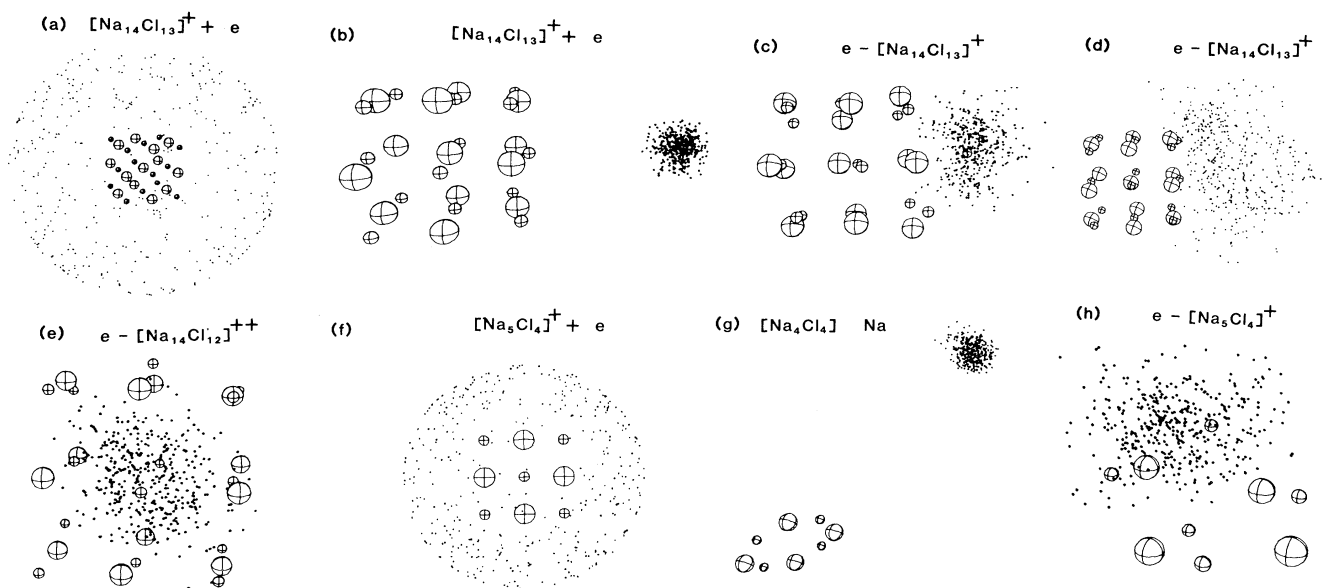


FIG. 1. Ionic configurations and "electron necklace" distributions for an excess electron interacting with sodium-chloride clusters. Small and large spheres correspond to  $\text{Na}^+$  and  $\text{Cl}^-$  ions, respectively. Dots represent 2D projections of the "electron beads." (a), (b) Alternate initial configurations of  $[\text{Na}_{14}\text{Cl}_{13}]^+ + e$  [in (b) the  $e$  bead is localized to the right of the cluster] which achieve the equilibrium configurations corresponding to surface states given in (c),  $R_c = 3.22a_0$ , and (d)  $R_c = 5.29a_0$ . (e) Equilibrium configuration of  $e$ - $[\text{Na}_{14}\text{Cl}_{12}]^{++}$ ,  $R_c = 3.22a_0$ , exhibiting an internal  $F$  center. (f) Initial state of  $e$ - $[\text{Na}_5\text{Cl}_4]^+$ . (g) Equilibrium configuration of  $e$ - $[\text{Na}_5\text{Cl}_4]^+$  with  $R_c = 3.22a_0$  resulting in dissociation of  $\text{Na}$ . (h) Equilibrium configuration of  $e$ - $[\text{Na}_5\text{Cl}_4]^+$  with  $R_c = 4.36a_0$  which corresponds to structural isomerization.

a.u.) exceeds the loss in  $E_c$  (0.0799 a.u.) favoring internal localization (Table I). It is of interest to note that the total energy of  $e\text{-}[\text{Na}_{14}\text{Cl}_{12}]^{++}$  is rather close to that of  $[\text{Na}_{14}\text{Cl}_{13}]^+$ , so that the electron binding energy in the cluster is similar to that of a negative ion, analogously to the situation for  $F$ -center formation in (extended) ionic crystals,<sup>8</sup> thus establishing the dominance of short-range attractive interactions in electron trapping (localization) phenomena. A drastically different localization mode is obtained in the  $e\text{-}[\text{Na}_{14}\text{Cl}_{13}]^+$  system [Fig. 1(c)], where a surface state is exhibited. For  $R_c = 3.22a_0$  the electron localizes around an  $\text{Na}^+$  surface ion [Fig. 1(c)], leaving an essentially neutral  $[\text{Na}_{13}\text{Cl}_{13}]$  cluster, which interacts with the (partially) neutralized Na atom mainly via polarization of the electron cloud (with a residual ionic binding of  $-0.002$  a.u.). We refer to this state as a cluster-surface localized state, which bears close analogy with Tamm's crystal-surface states.<sup>15</sup> When the pseudopotential cutoff  $R_c$  increases, the surface state becomes more extended [see Fig. 1(d) for  $R_c = 5.29a_0$ ] [the choice of an abnormally high value for  $R_c$  (i.e.,  $5.29a_0$ ) prevents internal localization in the  $[\text{Na}_{14}\text{Cl}_{12}]^{++}$  cluster since the internal region is then predominantly repulsive (see Table I), resulting in a surface state]. A measure of the spatial extent of the localized electron is given by the gyration radius of the "electron necklace"  $R^2 = (1/2p^2) \langle \sum_{i,j} (\mathbf{r}_i - \mathbf{r}_j)^2 \rangle$ , which demonstrates (Table I) the enhanced localization in the  $e\text{-}[\text{Na}_{14}\text{Cl}_{12}]^{++}$  system and the anisotropy of the electron distribution in the  $e\text{-}[\text{Na}_{14}\text{Cl}_{13}]^+$  system. An estimation of the extent of the electron thermal wave packet is obtained also by

$$R_T \equiv \left[ \frac{p}{p-1} \sum_{i=1}^p \langle (\mathbf{r}_i - \mathbf{r}_{i+1})^2 \rangle \right]^{1/2}$$

which for a free electron at room temperature yields  $R_T = \sqrt{3}\lambda_T \approx 56a_0$  ( $\lambda_T \approx 32.34a_0$ ). In all the calculations reported herein  $R_T$  values of  $52a_0$ – $55a_0$  were obtained, i.e., the same as the free-electron value to within statistical significance (compare to typical interionic distance of  $5a_0$  in NaCl clusters).

In smaller clusters novel effects of dissociative electron attachment and cluster isomerization induced by electron localization will be manifested. We have studied the smallest singly ionized cluster exhibiting high stability, i.e.,  $[\text{Na}_5\text{Cl}_4]^+$ , for which the lowest energy configuration is planar with four  $\text{Na}^+$  ions at the corners and one at the center of an approximate square.<sup>9</sup> This cluster possesses an isomeric structure (less stable by 0.014 a.u.) in which the ions are arranged in a distorted pyramidal configuration.<sup>9</sup> Adding

an electron to the ground-state planar configuration of  $[\text{Na}_5\text{Cl}_4]^+$  (with the  $\text{Na}^+$  pseudopotential being characterized by  $R_c = 3.22a_0$ ) transforms the system into a neutral  $[\text{Na}_4\text{Cl}_4]$  cluster with a planar ring structure and a dissociated neutral Na atom [Table I and Figs. 1(f) and 1(g), corresponding to the initial- and final-state configurations, respectively]. To demonstrate that this process is driven by the localization of  $e$  around a single  $\text{Na}^+$  ion, we have performed further simulations by decreasing the cation-electron binding strength, taking  $R_c = 4.36a_0$ . In this case, extreme localization is not sufficiently counterbalanced by  $e$  binding. Instead, the planar structure transforms to the isomeric pyramidal configuration with the electron localized as a diffuse cloud about the tip of the pyramid [Fig. 1(h)]. Electron localization accompanied by structural isomerization will constitute a prevalent phenomenon for AHC with smaller  $e$ -cation binding energy, i.e., the heavier alkali metals. In view of the intimate interrelationship between structural isomerization and melting of clusters,<sup>16</sup> it will be interesting to explore the melting of such finite systems induced by electron localization.

This work is supported by the U.S. Department of Energy under Contract No. EG-S-05-5489, and by the U.S. Army through its European Research Office.

<sup>1</sup>See papers in Ber. Bunsenges. Phys. Chem. **88** (1984).

<sup>2</sup>C. L. Briant and J. J. Burton, J. Chem. Phys. **63**, 2045 (1975).

<sup>3</sup>See review by F. F. Abraham, J. Vac. Sci. Technol. **82**, 534 (1984).

<sup>4</sup>J. Jortner, in Ref. 1, p. 188.

<sup>5</sup>D. Chandler and P. G. Wolynes, J. Chem. Phys. **79**, 4078 (1981).

<sup>6</sup>B. De Raedt, H. Sprik, and H. L. Klein, J. Chem. Phys. **80**, 5719 (1984).

<sup>7</sup>D. Chandler, J. Phys. Chem. **88**, 3400 (1984).

<sup>8</sup>M. Parrinello and A. Rahman, J. Chem. Phys. **80**, 860 (1984).

<sup>9</sup>T. P. Martin, Phys. Rep. **95**, 167 (1983).

<sup>10</sup>F. G. Fumi and M. P. Tosi, J. Phys. Chem. Solids **25**, 31, 45 (1964).

<sup>11</sup>R. W. Shaw, Phys. Rev. **174**, 769 (1968).

<sup>12</sup>L. S. Schulman, *Techniques and Applications of Path Integrals* (Wiley, New York, 1981).

<sup>13</sup>M. F. Herman, E. J. Bruskin, and B. J. Berne, J. Chem. Phys. **76**, 5150 (1982).

<sup>14</sup>D. Callaway and A. Rahman, Phys. Rev. Lett. **49**, 613 (1982).

<sup>15</sup>N. F. Mott and R. W. Gurney, *Electronic Processes in Ionic Crystals* (Oxford Univ. Press, Oxford, 1946).

<sup>16</sup>G. Natanson, F. Amar, and R. S. Berry, J. Chem. Phys. **78**, 399 (1983).